Physica B 407 (2012) 3229–3232

Contents lists available at SciVerse ScienceDirect

Physica B

journal homepage: www.elsevier.com/locate/physb

Study of the magnetic and structural properties of Mn-, Fe-, and Co-doped ZnO powder

Daniel A.A. Santos, Marcelo A. Macêdo *

Physics Department, Federal University of Sergipe, 49100-000 São Cristóvão, SE, Brazil

ARTICLE INFO

Available online 19 December 2011

Keywords:
Diluted magnetic semiconductors
ZnO
Proteic sol–gel process

ABSTRACT

A study of the magnetic and structural properties of $Zn_{1-x}M_xO$ powder (where $x=0$ or 0.01, and M=Mn, Fe or Co) produced by the proteic sol–gel process was undertaken. The sample crystal structure was analyzed by XRD and magnetic measurements were carried out in a SQUID magnetometer. Of the XRD analysis, all samples had hexagonal wurtzite crystal structure with P63mc space group, and no secondary phase was observed. It is observed of the $M(H)$ measures at 2 K, that the Co- and Mn-doped ZnO displayed saturation magnetizations (M_s) of approximately 2 and 3.2 emu/g, respectively, and no remanence (M_r) was observed, indicating a superparamagnetic behavior in these samples. However, the Fe-doped sample showed a ferromagnetic behavior with $M_s \sim 0.34$ emu/g, $M_r \sim 0.05$ emu/g, and coercivity (H_c) ~ 1090 Oe. Already at room temperature, the $M(H)$ measurements reveal a purely paramagnetic behavior for Mn- and Fe-doped ZnO, indicating that the Curie temperature (T_c) is below 300 K. However, a weak superparamagnetic behavior was observed in the Co-doped sample, indicating that $T_c > 300$ K.

1. Introduction

There is great interest in spintronics with semiconductors due to the possibility of combining their electrical and magnetic characteristics (i.e., current control by manipulation of spin, non-volatility), resulting in diluted magnetic semiconductors (DMS). Two materials intensively studied for DMS systems were GaMnAs [1,2] and InMnAs [3,4], however, their highest reported Curie temperatures (T_c) are only 170 K for GaMnAs and 35 K for InMnAs. Thus, there have been many research efforts into finding new DMS materials with Curie temperatures at or above room temperature to achieve a greater practical applicability. One of the most promising and extensively studied systems is transition-metal-doped ZnO [5]. However, there is heated debate regarding the ferromagnetism of this material, because several studies attribute this property to intrinsic phenomena [6,7], whereas others attribute it to extrinsic phenomena [8,9] and still others report the absence of this property in room temperature (300 K) transition-metal-doped ZnO [10,11]. Because of this controversy, many studies that argue intrinsic ferromagnetism in the transition-metal-doped ZnO in 300 K are not universally accepted. The problem of an extrinsic ferromagnet is that the possible limitations to its use in spintronics are unknown, such as, whether it is an effective spin injector [12]. Therefore, the origin of ferromagnetism in DMS must be understood for its applications to be most efficient. Thus, many open questions about transition-metal-doped ZnO must be answered. Why is the Curie temperature independent of the magnetic-element concentration? What is the mechanism behind doping with non-magnetic elements resulting in strong ferromagnetism? Why is the bulk nonmagnetic in some cases, whereas a thin film of the same composition is magnetic? How does the magnetic moment per cation exceed the limiting value established by Hund's rules or the time decay of the magnetization? Is the ferromagnetism caused by clusters, oxygen vacancies, distortions in the crystal lattice, holes in the valence band, or the insertion of magnetic polarons, or is it intrinsically due to doping? How do growth conditions influence the magnetism of the samples [13–23]. To contribute to a better understanding of transition-metal-doped ZnO, we present a study of the magnetic and structural properties of Mn-, Fe-, and Co-doped ZnO powders obtained from the proteic sol–gel process. This process consists in dissolving organic or inorganic salts in coconut water, followed by heat treatment. Coconut water is used to control the size of the crystals, by providing organic material that separates the ions in solution. So, the more diluted the solution, smaller will be the size of the crystals after heat treatment.

2. Experimental

The samples were prepared using the general reaction $(1-x)Zn(NO_3)_2 \cdot 6H_2O + xMQ \cdot yH_2O + CW \rightarrow Zn_{1-x}M_xO$, where $x=0$ for the pure oxide and $x=0.01$ for the doped oxide, M=Mn, Fe or

* Corresponding author. Tel.: +55 79 2105 6810; fax: +55 79 2105 6807.
E-mail address: mmacedo@ufs.br (M.A. Macêdo).

0921-4526
doi:10.1016/j.physb.2011.12.073

Co, Q=Cl_2 for Mn and Q=$(NO_3)_2$ for Fe and Co, y=4 for Mn, 9 for Fe and 6 for Co, and CW=coconut water. These solutions were put in a furnace for 24 h at 100 °C to eliminate excess water and form the xerogel. Next, the xerogel was calcinated at 1100 °C for 1 h to eliminate organic materials and form a powder. The crystalline phases were identified by X-ray diffraction (XRD) measurements with the Bragg–Brentano geometry through CuKα radiation using a Rigaku RINT 2000/PC diffractometer operating with 40 kV/40 mA in the 2θ range of 30°–70° with a step rate of 0.004°/s. The $M(H)$ and $M(T)$ magnetic measurements were carried out in a Quantum Design SQUID magnetometer MPMS-XL, using mass 50 mg of each sample.

3. Results and discussion

The XRD measurements of all samples revealed a wurtzite-type hexagonal crystalline structure with the P63mc space group and without spurious phases, as seen in [24]. Only the ZnO phase is present, which indicates either a total insertion of the dopant ions into the ZnO crystal lattice or a secondary phase that is so small that it is unobservable in XRD measurements. The $M(H)$ values at 2 and 300 K for the Mn- and Co-doped ZnO are shown in Figs. 1 and 2, respectively. In both cases, typical superparamagnetism behavior is observed at 2 K due to the absence of remanence (M_r) or coercivity (H_c), and the saturation magnetization (M_s) is approximately 3.2 emu/g for $Zn_{0.99}Mn_{0.01}O$ and 2 emu/g for $Zn_{0.99}Co_{0.01}O$. According to superparamagnetic theory [25], the magnetic relaxation time (τ) of a particle non-interactant in the zero field limit ($H\rightarrow 0$) is given by Eq. (1)

$$\tau = \tau_0 \exp(K_a V/k_B T) \quad (1)$$

where τ_0 is a factor related to the natural frequency of the gyromagnetic precession time and can be found theoretically or experimentally, K_a is the anisotropic energy density or anisotropy constant, V is the particle volume, k_B is the Boltzmann constant, and T is the absolute temperature. Therefore, according to Eq. (1), the thermal energy supplied (k_BT) to the $Zn_{0.99}Mn_{0.01}O$ and $Zn_{0.99}Co_{0.01}O$ samples at 2 K is sufficient to overcome the energy barrier (K_aV) and allow the rotation of the particle spins such that there is no remanence for H=0. In other words, the relaxation time of these particles is smaller than the measure time (t_m) at 2 K. In Fig. 1, a purely paramagnetic behavior is observed at 300 K, indicating that the Curie temperature (T_c) of this material is below room temperature. Whereas the included graph in Fig. 2 shows a weak superparamagnetic behavior at 300 K with an M_s value of approximately 0.0003 emu/g, indicating that T_c is above room temperature. Figs. 3 and 4 show the $M(T)$ curves of the $Zn_{0.99}Mn_{0.01}O$ and $Zn_{0.99}Co_{0.01}O$ samples under a DC field of 1000 Oe. Both samples demonstrate typical Langevin-paramagnetism behavior, in which the DC susceptibility ($\chi_{DC}=M/H_{DC}$) is a function that decreases rapidly with increasing temperature. In addition, no blocking temperature (T_B) is observed, which reinforces the argument made earlier that $\tau < t_m$ and that the particles are in the superparamagnetic state. However, both graphs of $\chi_{DC}^{-1}(T)$ (included in Figs. 3 and 4) obtained from ZFC curves show Langevin paramagnetic behavior (solid line) and Curie–Weiss ferromagnetic behavior (dashed line), indicating that the dopant ions of these samples also interact ferromagnetically with each other. However, the number of interacting atoms is so small that it was not possible to verify the remanence in the $M(H)$ curves at 2 K (Figs. 1 and 2), suggesting that the atoms of Mn and Co are well diluted in the ZnO matrix. A similar analysis was carried out by Martínez [26] to explain the antiferromagnetic behavior in a Co-doped ZnO sample. Fig. 5 shows $M(H)$ measurements of the Fe-doped ZnO at 2 and 300 K. Ferromagnetic behavior is observed at 2 K with M_s, M_r, and H_c values of approximately 0.34 emu/g, 0.05 emu/g, and 1090 Oe, respectively.

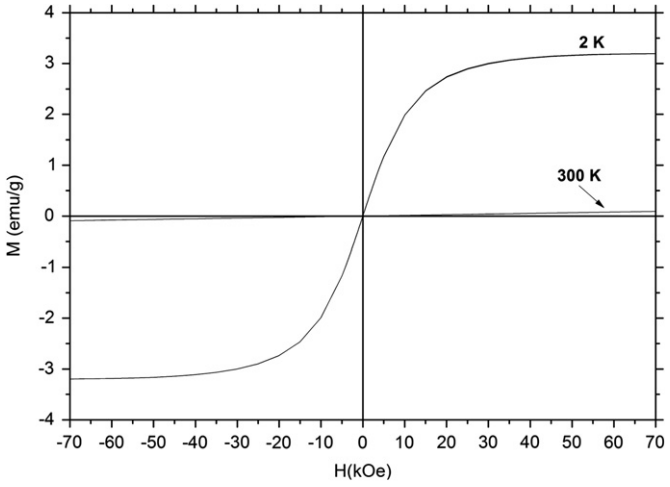

Fig. 1. $M(H)$ measurements at 2 and 300 K of the Mn-doped ZnO.

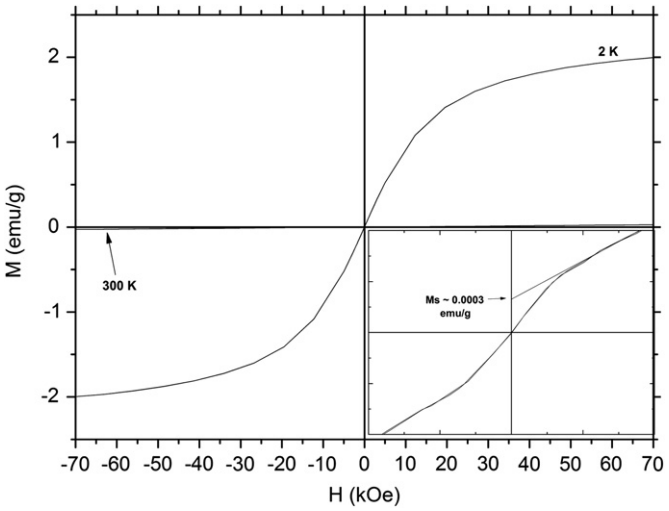

Fig. 2. $M(H)$ measurements at 2 and 300 K of the Co-doped ZnO. Inset: enlargement of the curve at 300 K showing $M_s \sim 0.0003$ emu/g.

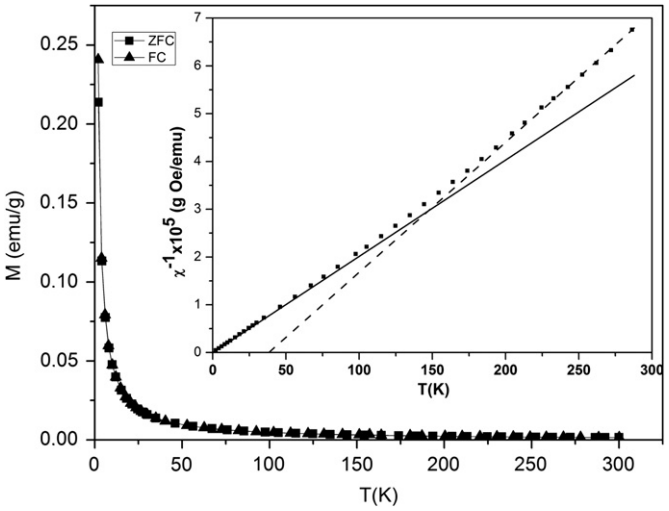

Fig. 3. $M(T)$ curves of the $Zn_{0.99}Mn_{0.01}O$ sample under a DC field of 1000 Oe. Inset: $\chi_{DC}^{-1}(T)$ graph obtained from ZFC curve.

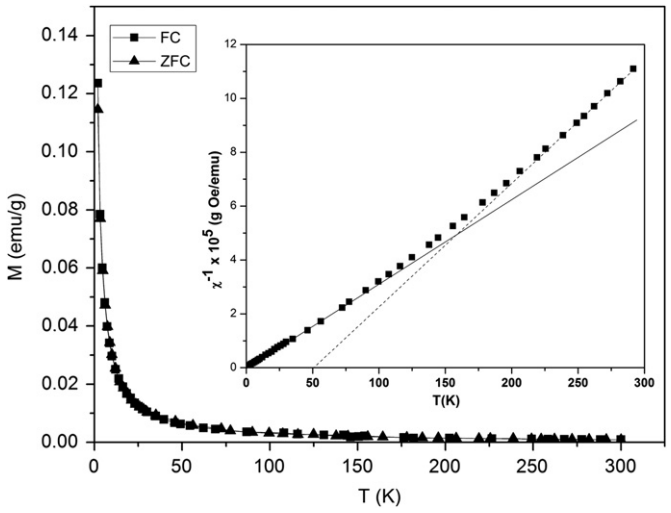

Fig. 4. $M(T)$ measurements of the $Zn_{0.99}Co_{0.01}O$ sample under a DC field of 1000 Oe. Inset: $\chi_{DC}^{-1}(T)$ graph obtained from ZFC curve.

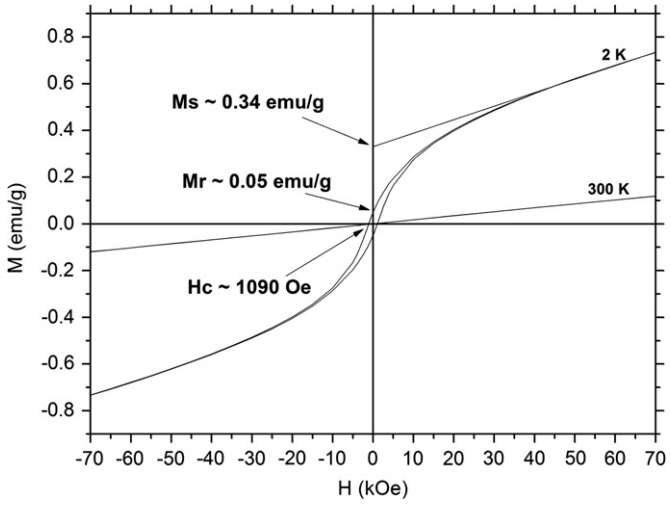

Fig. 5. $M(H)$ measurements at 2 and 300 K of the Fe-doped ZnO.

In this case, there are magnetic interactions between particles, which impede the rotation of spins and give rise to the remanence, in addition to the energy barrier K_aV (Eq. (1)). Thus, it is necessary to supply extra energy through the application of the coercive field H_c to demagnetize the material. Fig. 5 also shows purely paramagnetic behavior at 300 K, indicating that the Curie temperature (T_c) of this material is also below room temperature. Fig. 6 shows the $M(T)$ curve of the $Zn_{0.99}Fe_{0.01}O$ sample under a DC field of 1000 Oe. As expected, a blocking temperature ($T_B \sim 15$ K), characterized by a maximum in the ZFC curve, is observed, indicating a ferro-superparamagnetic or ferro-paramagnetic transition. In this case, T_B corresponds to the ferro-superparamagnetic transition because it is below T_c, however, if the two temperatures were equal, then it would correspond to the ferro-paramagnetic transition. In the $Zn_{0.99}Fe_{0.01}O$ sample, the particles are in the ferromagnetic state below T_B and are called blocked because the energy supplied is insufficient to allow the rotation of spins, and thus $\tau > t_m$. However, the particles are in the superparamagnetic state above T_B ($\tau < t_m$). Magnetic irreversibility temperature ($T_{irr} \sim 10$ K) is also observed, characterized by the separation of the ZFC and FC curves. This observation indicates either a spin glass behavior or the presence of secondary crystalline phases. However, the decrease in FC value with

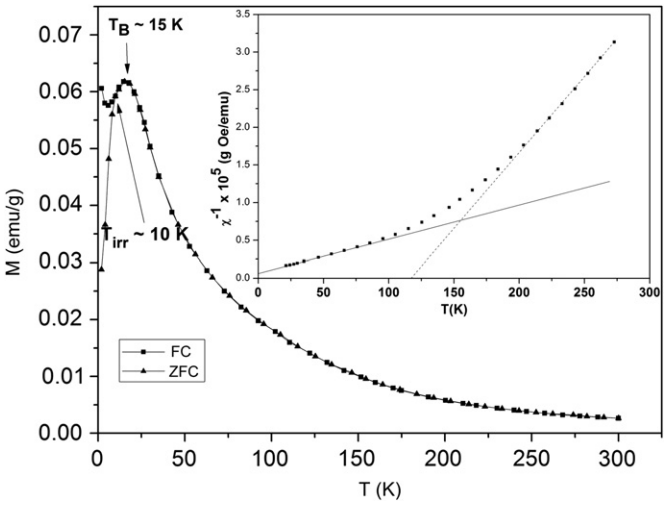

Fig. 6. $M(T)$ measurements of the $Zn_{0.99}Fe_{0.01}O$ sample under a DC field of 1000 Oe, showing the blocking ($T_B \sim 15$ K) and irreversibility ($T_{irr} \sim 10$ K) temperatures. Inset: $\chi_{DC}^{-1}(T)$ graph obtained from ZFC curve.

decreasing temperature (Fig. 6) from 15 to 10 K (i.e., T_B to T_{irr}) suggests the presence of a small antiferromagnetic phase not visible in the XRD analysis. This finding is confirmed by the analysis of the graphs $\chi_{DC}^{-1}(T)$ (inset in Fig. 6), which shows Curie–Weiss antiferromagnetic (solid line) and ferromagnetic (dashed line) behavior. Therefore, total insertion of the Fe ions in the ZnO crystal lattice does not occur, leading to the formation of a small secondary antiferromagnetic phase (e.g., Fe_2O_3 or FeO), which explains the low M_s value of this sample.

4. Conclusion

All samples had hexagonal wurtzite crystal structures with the P63mc space group and no secondary phase, as observed via XRD. At 2 K the Co- and Mn-doped ZnO presented a superparamagnetic behavior, whereas the Fe-doped sample showed a ferromagnetic behavior. However, at 300 K, the Mn- and Fe-doped ZnO revealed a purely paramagnetic behavior indicating that T_c is below room temperature and the Co-doped sample showed a weak superparamagnetic behavior (i.e., $T_c > 300$ K). A detailed magnetic analysis suggests the presence of small spurious antiferromagnetic phase in the $Zn_{0.99}Fe_{0.01}O$ sample, which was not observed via XRD.

Acknowledgments

The authors acknowledge CNPq for financial assistance.

References

[1] H. Ohno, A. Shen, F. Matsukura, A. Oiwa, A. Endo, S. Katsumoto, Y. Iye, Appl. Phys. Lett. 69 (1996) 363.
[2] K. Ando, T. Hayashi, M. Tanaka, A. Twardowski, J. Appl. Phys. 83 (1998) 65481.
[3] H. Munekata, H. Ohno, S. von Molnar, A. Segmuller, L.L. Chang, L. Esaki, Phys. Rev. Lett. 63 (1989) 1849.
[4] H. Munekata, A. Zaslevsky, P. Fumagalli, R.J. Gambino, Appl. Phys. Lett. 63 (1993) 2929.
[5] Ü. Ozgur, et al., J. Appl. Phys. 98 (2005) 41301.
[6] J.M.D. Coey, M. Venkatesan, C.B. Fitzgerald, Nat. Mater. 4 (2005) 173.
[7] He Wei, et al., J. Appl. Phys. 105 (2009) 043903.
[8] J.H. Park, M.G. Kim, H.M. Jang, S.W. Ryu, Y.M. Kim, Appl. Phys. Lett. 84 (2004) 1338.
[9] Q. Liu, C.L. Gan, C.L. Yuan, G.C. Han, Appl. Phys. Lett. 92 (2008) 032501.

[10] D.P. Norton, et al., Appl. Phys. Lett. 83 (2003) 5488.
[11] A. Ney, et al., Phys. Rev. Lett. 100 (2008) 157201.
[12] I. Zutic, J. Fabian, S. Das Sarma, Rev. Mod. Phys. 76 (2004).
[13] S.A. Chambers, Surf. Sci. Rep. 61 (2006) 345.
[14] P. Sati, et al., Phys. Rev. Lett. 98 (2007) 137204.
[15] Q. Xu, et al., Appl. Phys. Lett. 92 (2008) 082508.
[16] C.H. Patterson, Phys. Rev. B 74 (2006) 144432.
[17] C. Song, et al., Phys. Rev. B 73 (2006) 24405.
[18] A.J. Behan, et al., Phys. Rev. Lett. 100 (2008) 47206.
[19] N.H. Hong, et al., Phys. Rev. B 72 (2005) 45336.
[20] J.M.D. Coey, J. Appl. Phys. 97 (2005) 10D313.
[21] A. Che Mofor, et al., Appl. Phys. Lett. 87 (2005) 62501.
[22] A.S. Risbud, et al., Phys. Rev. B 68 (2003) 205202.
[23] M.A. García, et al., NanoLetters 7 (2007) 1489.
[24] D.A.A. Santos, A.D.P. Rocha, M.A. Macêdo, Powder Diffr. 23 (2008) 2.
[25] C.P. Bean, J.D. Livingston, J. Appl. Phys. 30 (1959) 120.
[26] B. Martínez, Phys. Rev. B 72 (2005) 165202.